MATHEMATICAL BIOSCIENCES
AND ENGINEERING
Volume **9**, Number **3**, July **2012**

doi:10.3934/mbe.2012.9.663

pp. **663–683**

A MINIMAL MATHEMATICAL MODEL FOR THE INITIAL MOLECULAR INTERACTIONS OF DEATH RECEPTOR SIGNALLING

Christian Winkel

Institute of Applied Analysis and Numerical Simulation, Univ. of Stuttgart
Pfaffenwaldring 57, 70569 Stuttgart, Germany

Simon Neumann

Institute of Cell Biology and Immunology, Univ. of Stuttgart
Allmandring 31, 70569 Stuttgart, Germany

Christina Surulescu

Institute of Computational and Applied Mathematics, WWU Münster
Einsteinstr. 62, 48149 Münster, Germany

Peter Scheurich

Institute of Cell Biology and Immunology, Univ. of Stuttgart
Allmandring 31, 70569 Stuttgart, Germany

(Communicated by Haiyan Wang)

Abstract. Tumor necrosis factor (TNF) is the name giving member of a large cytokine family mirrored by a respective cell membrane receptor super family. TNF itself is a strong proinflammatory regulator of the innate immune system, but has been also recognized as a major factor in progression of autoimmune diseases. A subgroup of the TNF ligand family, including TNF, signals via so-called death receptors, capable to induce a major form of programmed cell death, called apoptosis. Typical for most members of the whole family, death ligands form homotrimeric proteins, capable to bind up to three of their respective receptor molecules. But also unligated receptors occur on the cell surface as homomultimers due to a homophilic interaction domain. Based on these two interaction motivs (ligand/receptor and receptor/receptor) formation of large ligand/receptor clusters can be postulated which have been also observed experimentally. We use here a mass action kinetics approach to establish an ordinary differential equations model describing the dynamics of primary ligand/receptor complex formation as a basis for further clustering on the cell membrane. Based on available experimental data we develop our model in a way that not only ligand/receptor, but also homophilic receptor interaction is encompassed. The model allows formation of two distict primary ligand/receptor complexes in a ligand concentration dependent manner. At extremely high ligand concentrations the system is dominated by ligated receptor homodimers.

2000 *Mathematics Subject Classification.* Primary: 92C37.

Key words and phrases. Tumor necrosis factor, death receptor, ligand/receptor clustering, ODE model, stability analysis, homomultimers.

The authors would like to thank the German Research Foundation (DFG) for the financial support of the project within the Cluster of Excellence in Simulation Technology (EXC 310/1) at the University of Stuttgart.

1. **Introduction.** Responses of the immune system are tightly regulated among others by soluble factors called cytokines. One major cytokine family is the tumor necrosis factor (TNF) ligand family. Most TNF ligand family members are primarily produced as bioactive type II transmembrane proteins but also exist as soluble factors. Their interaction partners, represented by the TNF receptor superfamily, also show considerable homologies in their extracellular domains and are mainly expressed in immune cells but also in other tissues [1]. A subgroup of the TNF ligand family comprises the so-called death ligands, including TNF itself and the ligands TRAIL (TNF related apoptosis-inducing ligand) and FasL (Fas ligand). Death receptors have the capability to activate the cellular program of apoptosis, a major form of programmed cell death and an important physiological process to remove infected, malfunctioning, or no longer needed cells from multicellular organisms. Besides its apoptotic capabilities TNF is a prominent regulator of inflammation and innate immune responses, but also plays a key role in progression of autoimmune diseases like rheumatoid arthritis, Crohn's disease and psoriasis. Therefore it constitutes an important therapeutic target. Most membrane bound and soluble TNF family ligands form stable, non-covalently linked homotrimers capable to bind up to three of their respective receptor molecules in the grooves between their individual monomers [3, 15, 22]. Originally it was assumed that unligated receptors freely diffuse as monomers in the plasma membrane and become trimerized by binding to their ligand for initiation of intracellular signaling. Accordingly, ligand/receptor signaling complexes were believed to comprise a single ligand homotrimer bound with three receptor molecules. Several experimental findings, however, question this hypothesis. In different experimental systems the formation of large ligand/receptor clusters has been observed [13, 28] and cluster formation has been shown to be tightly correlated with efficient signal induction [17]. Structural analysis of the intracellular signaling part of the apoptotic receptor Fas complexed with its cytoplasmic adapter protein FADD (Fas associated death domain) also revealed higher ordered ring-like complexes containing five to seven copies of each interacting protein [34]. In addition, many members of the TNF receptor family are largely unresponsive to their soluble homotrimeric ligands, but strongly respond to the respective membrane bound preforms [2, 11, 21, 26]. However, unresponsiveness to the soluble ligands can generally be overcome by using ligand mutants engineered to form higher multimers of the respective ligand homotrimers [4, 14, 17, 32]. Together, these data suggest that ligand binding to their respective membrane receptors induces formation of larger clusters, representing the actual inducers of intracellular signaling.

New light was shed on the TNF receptor family when it was demonstrated that TNF receptors, as well as additional family members including the four human TRAIL receptors and Fas, possess a homophilic interaction domain, called preligand binding assembly domain (PLAD), being located in the extracellular most membrane distal part of the molecules [7, 8, 27]. Originally, PLAD-mediated formation of receptor homotrimers was proposed, but own experimental data strongly favor preferential homodimer formation in accordance with crystallization studies of the extracellular domain of TNFR1 [23]. In addition we have presented evidence that both molecular interactions, ligand/receptor interaction and PLAD-mediated receptor/receptor interaction, take place in the formation of ligand receptor clusters [6]. Taking homodimerization of unligated receptors into account two distinct mechanisms of initial ligand/receptor interaction can be proposed as discussed in detail in [5]. As homodimerized receptors expressed at the cell surface are assumed to have accessible ligand interaction sites [24], in the very first binding step one of the dimerised receptor molecules will interact with its ligand trimer as schematically depicted in Fig. 1. In the next step two alternatives are feasible. Either the homophilic receptor interaction can be opened to allow the second receptor chain to also bind the ligand. The resulting primary complex now consists of a single TNF homotrimer having two receptor chains bound at two of its three interaction sites, thereby not allowing any interactions between these two receptors (complex c_4 in Fig. 5). In this case avidity effects might control the overall reaction, because two receptor chains now simultaneously interact with a single TNF homotrimer. Alternatively, an additional TNF molecule will bind to the receptor without opening the homophilic receptor/receptor interaction (complex c_3 in Fig. 1). No avidity effects take place in this case. As the ratio of the two interaction partners are different in both complexes (c_3: two ligand trimers bind two receptors; c_4: one ligand trimer binds two receptors), high ligand concentrations must favor c_4 formation. In any case, under physiological conditions these differentially formed primary complexes would then interact with each other while diffusing in the plasma membrane and eventually reorganize to form larger clusters having a 1:3 stoichiometry (i.e. one homotrimer of the ligand is bound to three receptor chains).

This paper is organized as follows: in the next section we develop our model for the formation of elementary ligand/receptor complexes which are able to initiate intracellular signaling processes and provide an insight into the stability properties of the model. In section 3 we present the results of numerical simulations for different receptor and ligand concentrations when varying relevant reaction constants. In the conclusions we make an assessment of the different approaches to receptor crosslinking behaviour outlining the observation that initial homodimeric receptor formation leads to a saturation process in receptor-ligand binding.

2. **Modelling.**

In this section we develop a model for the first steps in the interaction of the TNF homotrimer with its receptor homodimers, representing an example of ligand/receptor interaction for most members of these families in general, according to our hypotheses as stated above.

Thereby we proceed by firstly introducing and analysing a model that is substantially based on facts available in the literature and allows us to draw conclusions on equilibrium concentrations of elementary receptor/ligand aggregates (in the case of ligand excess). We then extend this model by including another possible ligand/receptor configuration with mostly unknown constraints and investigate the impact of this new complex on the overall behaviour of the system.

2.1. **First model.**

For the description of our minimal model we rely on a typical setting of a cell death assay, where the initial ligand binding step can also be carried out at a temperature of 0 °C in order to exclude movement in the membrane. Moreover, we consider a homogeneous membrane with uniformly distributed receptors, which on its part renders the issue of spatiality irrelevant.

Figure 1 illustrates the reactions accounted for. We assume that at the starting point $t = 0$ of the reactions all ligand is unbound and all receptors exist in an equilibrium state between monomers and the parallel arranged homodimers. The former correspond to the leftmost part of Figure 1 and are in equilibrium with the parallel arrangement as characterised by the forward and reverse reaction rates k_1 and k_{-1}, respectively. When ligand becomes available the next step in the reaction is its binding to the extracellular domain of one of the receptors, which results in the complex denoted by c_2. Again, k_2 and k_{-2} denote the forward and reverse reaction rates. The final step in this model consists in the binding of another ligand to the remaining free receptor in the complex c_2, thus forming the receptor-ligand aggregate c_3. At this point two scenarios seem possible. Either the complex c_3 is signalling competent and enables a signal whose strength is correlated to the concentration of c_3 or in the case of a signalling dead end substrate inhibition could be expected. Further steps not considered here could lead to the formation of larger clusters.

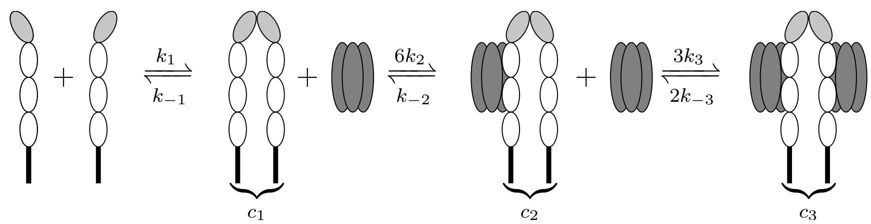

FIGURE 1. Formation of the receptor complex c_1 and the receptor/ligand complexes c_2 and c_3.

Relying on mass action kinetics we deduce a set of equations describing the evolution of the different receptor/ligand complexes:

$$
\begin{aligned}
\frac{dl}{dt} &= k_{-2}c_2 + 2k_{-3}c_3 - 6k_2c_1l - 3k_3c_2l, && l(0) = l_0,\\
\frac{dc_1}{dt} &= k_1r^2 + k_{-2}c_2 - k_{-1}c_1 - 6k_2c_1l, && c_1(0) = 0,\\
\frac{dc_2}{dt} &= 6k_2c_1l + 2k_{-3}c_3 - k_{-2}c_2 - 3k_3c_2l, && c_2(0) = 0,\\
\frac{dc_3}{dt} &= 3k_3c_2l - 2k_{-3}c_3, && c_3(0) = 0.
\end{aligned} \tag{1}
$$

Revisiting our previous comments on spatiality we assume that the location of receptors is constant. Regarding now the time frame relevant for the model it is important to point out that receptor synthesis and degradation are comparably slow processes with receptor half life being in the order of 3 hours. Taking furthermore into account that internalisation of the signaling complexes has a half life in the order of 20 minutes, the association rate of the ligand in comparison to these processes is high (see [12]) and half maximal binding typically occurs in less than one minute. These considerations allow neglecting the effects of synthesis, degradation and internalization of receptors. Hence, the following conservation law can be written for the total concentration of receptors r_T in terms of free receptors r and receptors bound in the corresponding complexes:

$$r_T = r + 2c_1 + 2c_2 + 2c_3. \tag{2}$$

Before starting to investigate the model's properties we would like to stress out again that we only consider steady state configurations of the system (1), since the formation of complexes on the cell surface happens very fast, as explained above. Secondly, we assume that no binding site on the ligands and the receptors is favoured, which leads to the integer multiples in front of the reaction rates accounting for the number of equivalent configurations of the possible receptor/ligand complexes. Thirdly, in contrast to previous research, in our model the forming of the homodimeric receptor complexes is crucial for initiating the clustering and signalling process and cannot be achieved by a complex consisting of less than two receptors.

Nondimensionalisation. In order to simplify the analysis of the model it is convenient to eliminate the physical dimensions of the involved quantities. Thus we define the complexes C_1, C_2, C_3, ligands L and receptors R by introducing the scaling constant C_0 that will be in the range of a typical ligand concentration used during experiments and derive the dimensionless time τ by additionally coupling it to the reaction rate k_1:

$$\tau = k_1 C_0 t, \quad C_1 = \frac{c_1}{C_0}, \quad C_2 = \frac{c_2}{C_0}, \quad C_3 = \frac{c_3}{C_0}, \quad L = \frac{l}{C_0}, \quad R = \frac{r}{C_0}. \tag{3}$$

Then the following notations

$$K_1 := \frac{6k_2}{k_1},\ K_2 := \frac{3k_3}{k_1},\ K_3 := \frac{k_{-1}}{k_1 C_0},\ K_4 := \frac{k_{-2}}{k_1 C_0},\ K_5 := \frac{2k_{-3}}{k_1 C_0} \tag{4}$$

lead to the dimensionless formulation of the system (1) and the conservation law for the receptors (2) to be used throughout the rest of this paper:

$$\begin{aligned}
\frac{dL}{d\tau} &= K_4 C_2 + K_5 C_3 - K_1 C_1 L - K_2 C_2 L,\\
\frac{dC_1}{d\tau} &= R^2 + K_4 C_2 - K_3 C_1 - K_1 C_1 L,\\
\frac{dC_2}{d\tau} &= K_1 C_1 L + K_5 C_3 - K_4 C_2 - K_2 C_2 L,\\
\frac{dC_3}{d\tau} &= K_2 C_2 L - K_5 C_3
\end{aligned} \tag{5}$$

and

$$R_T = R + 2C_1 + 2C_2 + 2C_3 \quad \text{with} \quad R_T := \frac{r_T}{C_0}. \tag{6}$$

Stability. After having deduced the nondimensional formulation of our model we are interested in the stability properties of the system (5), but before that we address the important positivity issue for the solution of the system, which is summarised in the following

Lemma 2.1 (Invariance of the first orthant)**.** *For a non-negative parameter set $K_1, \ldots, K_5$ and non-negative initial conditions the solution of the system (5) together with the conservation law (6) remains positive for all times $t \geq 0$.*

Proof. For our proof we follow the ideas presented in [29] and [33]. We show that any trajectory starting in the first orthant can never cross any bounding hyperplane. Let $K_1, \ldots, K_5$ be a set of non-negative parameters and consider a trajectory inside the first orthant approaching consecutively each of the bounding hyperplanes:

(i) $L = 0$: $\frac{dL}{d\tau} = \underbrace{K_4 C_2}_{\geq 0} + \underbrace{K_5 C_3}_{\geq 0} - \underbrace{K_1 C_1 L}_{=0} - \underbrace{K_2 C_2 L}_{=0} \geq 0,$

(ii) $C_1 = 0$: $\frac{dC_1}{d\tau} = \underbrace{R^2}_{\geq 0} + \underbrace{K_4 C_2}_{\geq 0} - \underbrace{K_3 C_1}_{=0} - \underbrace{K_1 C_1 L}_{=0} \geq 0,$

(iii) $C_2 = 0$: $\frac{dC_2}{d\tau} = \underbrace{K_1 C_1 L}_{\geq 0} + \underbrace{K_5 C_3}_{\geq 0} - \underbrace{K_4 C_2}_{=0} - \underbrace{K_2 C_2 L}_{=0} \geq 0,$

(iv) $C_3 = 0$: $\frac{dC_3}{d\tau} = \underbrace{K_2 C_2 L}_{\geq 0} - \underbrace{K_5 C_3}_{=0} \geq 0.$

Summing up we find that on every bounding hyperplane the vector field is pointing inward the first orthant, which justifies its invariance. □

Next we examine the stability of the system. As a first step we compute the steady states upon solving for $\frac{dL}{d\tau} = 0$, $\frac{dC_i}{d\tau} = 0$ $(i = 1, 2, 3)$. This results in:

$$C_1 = \frac{R^2}{K_3}, \qquad C_2 = \frac{K_1}{K_3 K_4} L R^2, \qquad C_3 = \frac{K_1 K_2}{K_3 K_4 K_5} L^2 R^2. \tag{7}$$

In order to eliminate the free variables R and L we consider the conservation equation (6) for the receptor concentration and find additionally by summing up the first, third and fourth equations of the system (5) another conservation law for the ligand concentration:

$$0 = \frac{dL}{dt} + \frac{dC_2}{dt} + 2\frac{dC_3}{dt} \implies L_T = L + C_2 + 2C_3 \quad \text{with} \quad L_T := L(0). \tag{8}$$

Substituting the computed equilibrium points for C_1, C_2 and C_3 in (6) and (8) then yields the following nonlinear system of equations for the steady state concentrations of receptors and ligands, respectively:

$$\begin{aligned} 2R^2 \left(\frac{K_1 K_2}{K_3 K_4 K_5} L^2 + \frac{K_1}{K_3 K_4} L + \frac{1}{K_3} \right) + R - R_T = 0, \\ 2L^2 \frac{K_1 K_2 R^2}{K_3 K_4 K_5} + L \left(1 + \frac{K_1 R^2}{K_3 K_4} \right) - L_T = 0. \end{aligned} \tag{9}$$

Solving these quadratic equations either for R or L and setting $K_c := K_3 K_4 K_5$ we obtain

$$L_{1,2} = -\frac{K_c + K_1 K_5 R^2 \pm \sqrt{(K_c)^2 + 2K_1 (K_c K_5 + 4K_2 K_c L_T) R^2 + (K_1 K_5)^2 R^4}}{4K_1 K_2 R^2},$$

$$R_{1,2} = -\frac{K_c \mp \sqrt{(K_c)^2 + 8K_c K_4 K_5 R_T + 8K_1 K_c K_5 R_T L + 8K_1 K_2 K_c R_T L^2}}{4(K_4 K_5 + K_1 K_5 L + K_1 K_2 L^2)}.$$

Given this system we now choose our parameter set for the further analysis of our model as follows:

$$K_1 = 13\,000, \quad K_2 = 6\,500, \quad K_3 = 500, \quad K_4 = 125 \quad \text{and} \quad K_5 = 250. \tag{10}$$

These values arise from the choice of the reaction constants according to literature data (see [12, 20]) as shown in Table 2 with $K_{D_1} = 10^{-6}$ M and $C_0 = 2 \times 10^{-9}$ M (typical ligand concentration). Figure 2 shows the null clines of the system (9) and their intersections for fixed total receptor concentration R_T and fixed total ligand concentration L_T. While the left-hand side displays two intersections located in the III. and in the IV. quadrant the right-hand side shows three intersections, one again in the IV. quadrant, another in the II. quadrant and yet another one in the I. quadrant, the latter being the only physically relevant solution.

In order to further examine the stability of the steady states we use linearisation theory and compute the eigenvalues of the Jacobian (11) in every steady state associated to the solutions of system (9). These calculations are presented in Table

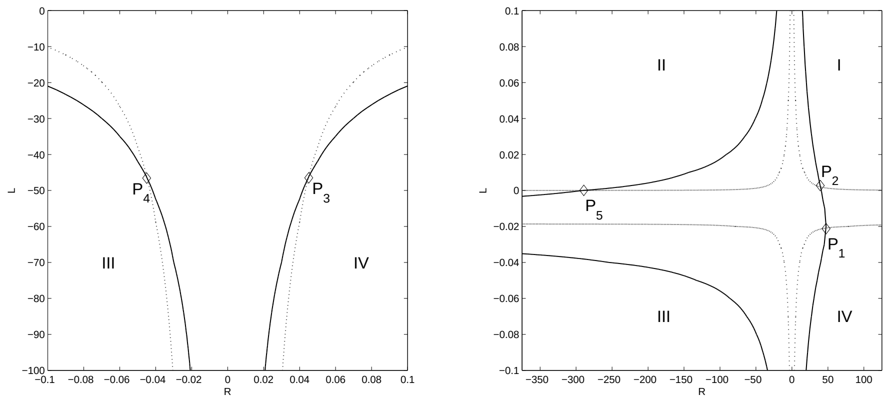

(a) Intersections in the III. and IV. quadrant

(b) Intersections in the I., II. and IV. quadrant

FIGURE 2. Null clines of the system of equations (9) for $R_T = 47.5$ and $L_T = 1$.

1. Notice that there exist one positive stable and one negative stable steady state, which are separated by at least one unstable steady state

$$\mathrm{J} = \begin{pmatrix} -K_1C_1 - K_2C_2 & -K_1L & K_4 - K_2L & K_5 \\ -K_1C_1 & -K_1L - K_3 & K_4 & 0 \\ K_1C_1 - K_2C_2 & K_1L & -K_2L - K_4 & K_5 \\ K_2C_2 & 0 & K_2L & -K_5 \end{pmatrix}. \tag{11}$$

Solutions			Eigenvalues			
	R	L	Re(λ_1)	Re(λ_2)	Re(λ_3)	Re(λ_4)
P_1	+4.7e+01	−2.1e−02	+6.2e+03	−3.3e+02	−3.3e+02	+1.9e−14
P_2	+3.9e+01	+2.7e−03	−4.6e+04	−1.3e−14	−5.1e+02	−2.8e+02
P_3	+4.5e−02	−4.6e+01	+3.0e+05	+6.0e+05	+8.9e−05	+8.9e−12
P_4	−4.5e−02	−4.7e+01	+3.0e+05	+6.0e+05	+8.9e−05	+1.5e−11
P_5	−2.9e+02	+5.7e−05	−2.2e+06	−1.8e−14	−5.0e+02	−2.5e+02

TABLE 1. Solutions to the system (9) and eigenvalues of the associated steady states.

Figure 3 illustrates the results of a numerical simulation of the system (5) with fixed non-negative initial data for R_T and L_T and the corresponding steady states. Clearly, the convergence to the steady state in each component of system (5) can be noted.

However, since we are interested in the behaviour of the system for a broader range of initial conditions for R_T and L_T we perform in a next step a bifurcation analysis with these parameters. For the moment assume that the two parameters cannot change their values simultaneously; hence we fix one at a time and calculate all (real) steady state solutions to (5) as a function of R_T and L_T, respectively. Considering the fact that these steady states are actually 5-dimensional vectors of the form (R, L, C_1, C_2, C_3) we decided to assess the characteristics of system (5) by merely plotting the (orthogonal projection on the) R component, which enables performing a qualitative analysis w.r.t. the number of steady-states, their stability and positivity.

We start by setting $L_T = 1$ and varying R_T in the range of 4.75×10^{-6} up to 4.75×10^{3}. The results of these calculations are displayed in the Subfigures (a) and (c) of Figure 4. There, the component R of the steady solution vector for the complete system (5) is plotted against R_T with $R > 0$ being drawn in Subfigure (a) and $R < 0$ being displayed in Subfigure (c) due to the log-log scale plot (with the convention that the ticks of the axes are labeled with the unscaled data). The annotations "negative" and "positive" given by the legend express the positivity of the complete steady state vector being meant componentwise and the negativity of at least one component of the steady state vector, respectively. Further on we use standard notation in order to discern stable and unstable steady states implying that the dashed lines indicate an unstable and the solid lines a stable state. So we find that the system for the considered configuration possesses only one positive stable steady state.

The same behaviour can be observed in the Subfigures (b) and (d) showing the results of the steady state calculations, this time only with $R_T = 47.5$ and L_T varying in the range of 10^{-6} to 10^{3}. Similarly to the plots in the Subfigures (a) and (c) here the value of the component R of the steady solution vector is plotted against L_T with $R > 0$ like before in the upper drawing and $R < 0$ in the lower chart due to the log-log scale plot. As already mentioned we can find analogously to the previous case two stable steady states that are separated by at least one unstable steady state. However, in either case the negative steady states cannot be reached by starting with non-negative initial conditions, thus confirming our previous results.

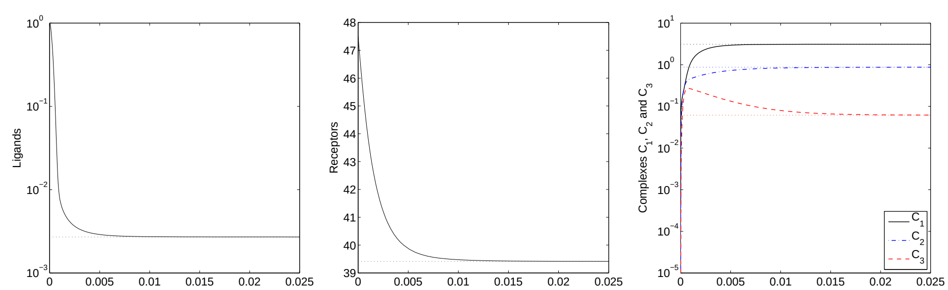

(a) Ligand concentration (b) Receptor concentration (c) Concentration of C_1, C_2 and C_3

FIGURE 3. Regime of the different nondimensional concentrations and the corresponding steady states (dotted lines) for $R_T = 47.5$ and $L_T = 1$.

2.2. **Model extension.** Having developed and analysed a model largely based on data available in the literature we now aim to extending it by adding another

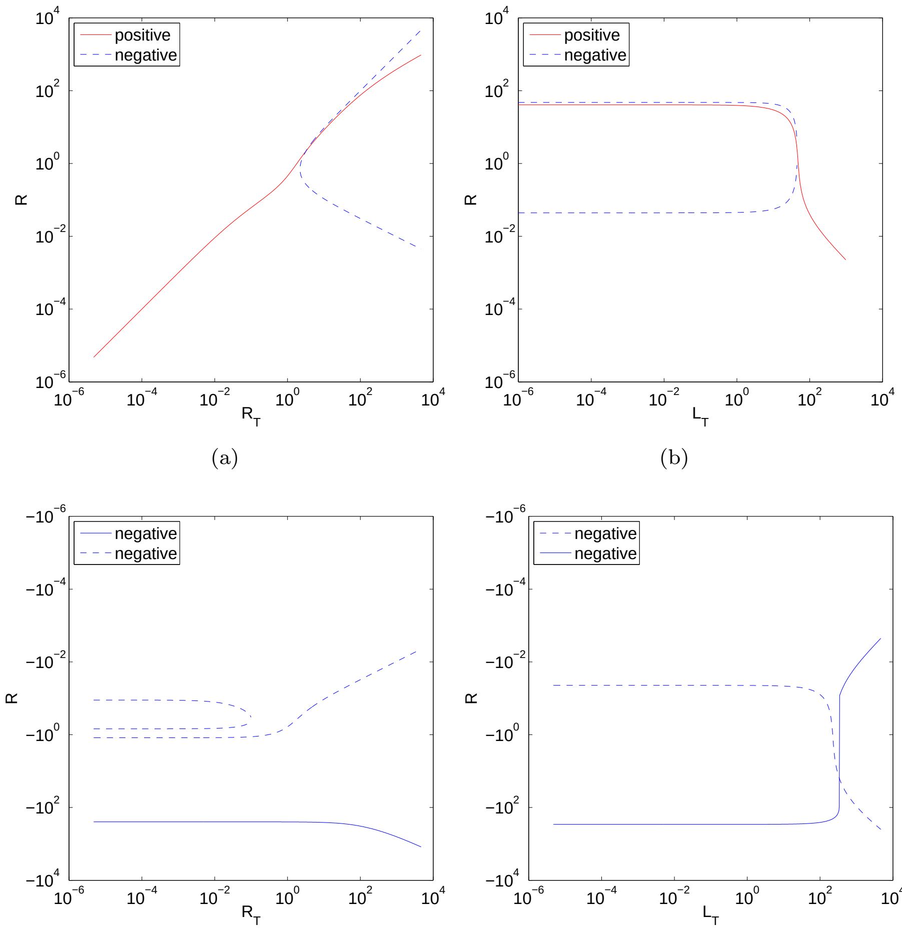

(a) (b) (c) (d)

FIGURE 4. Bifurcation diagram for fixed ligand concentration and varying receptor concentration (subfigures (a) and (c)) and for varying ligand and fixed receptor concentration (subfigures (b) and (d)). Solid and dashed lines indicate the stability and instability of a steady state, while the colours red and blue denote its positivity and negativity, respectively (log-log plot).

possible receptor/ligand configuration (encircled with the dashed line in Figure 5) with constraints that are not well known. Therefore we consider the system at the point when it has already formed complex c_2 and introduce another possible configuration. This means that complex c_2 now has not only the possibility to bind another ligand but also to open its homophilic bond and rearrange itself by binding both receptors to the ligand. As before we characterise this reaction with the forward and reverse reaction rates k_4 and k_{-4}, respectively.

Since most of the calculations for the expanded model will be similar to those presented in the previous section, we will focus on showing only the most important steps.

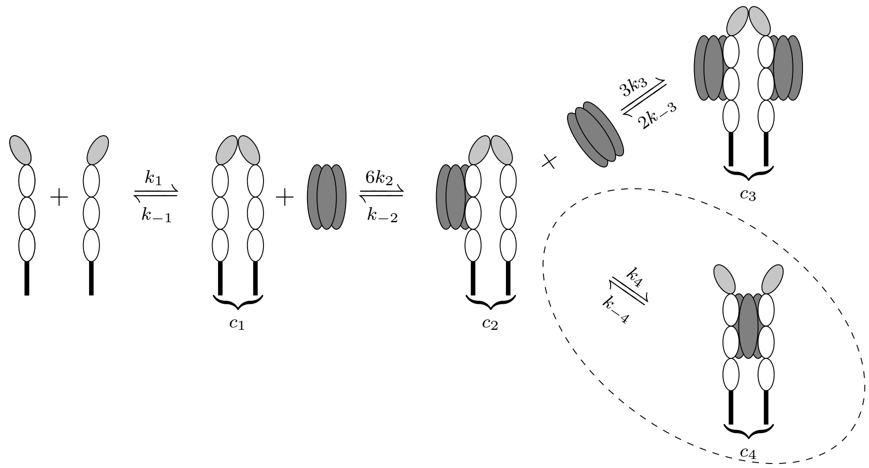

FIGURE 5. Formation of the receptor complex c_1 and the receptor/ligand complexes c_2, c_3 and c_4

Relying again on mass actions kinetics we find the set of equations consisting of the system (1) complemented by the interactions of c_2 with the additional receptor/ligand complex c_4

$$\begin{aligned}
\frac{dl}{dt} &= k_{-2}c_2 + 2k_{-3}c_3 - 6k_2c_1l - 3k_3c_2l, && l(0) = l_0,\\
\frac{dc_1}{dt} &= k_1r^2 + k_{-2}c_2 - k_{-1}c_1 - 6k_2c_1l, && c_1(0) = 0,\\
\frac{dc_2}{dt} &= 6k_2c_1l + 2k_{-3}c_3 + k_{-4}c_4 - k_{-2}c_2 - k_4c_2 - 3k_3c_2l, && c_2(0) = 0,\\
\frac{dc_3}{dt} &= 3k_3c_2l - 2k_{-3}c_3, && c_3(0) = 0,\\
\frac{dc_4}{dt} &= k_4c_2 - k_{-4}c_4, && c_4(0) = 0.
\end{aligned} \tag{12}$$

Imposing the same constraints on the time frame considered like in the previous section lets us consequently deduce the conservation law for the total receptor concentration in terms of unbound monomeric receptors and receptors bound in the complexes c_1 to c_4

$$r_T = r + 2c_1 + 2c_2 + 2c_3 + 2c_4. \tag{13}$$

Nondimensionalisation. In order to reduce the number of free parameters in the expanded model we proceed in a similar way by nondimensionalising the given quantities by the scaling constant C_0 and reaction rate k_1:

$$\tau = k_1C_0t,\ C_1 = \frac{c_1}{C_0},\ C_2 = \frac{c_2}{C_0},\ C_3 = \frac{c_3}{C_0},\ C_4 = \frac{c_4}{C_0},\ L = \frac{l}{C_0},\ R = \frac{r}{C_0}. \tag{14}$$

This allows us to formulate the following dimensionless coefficients whose insertion into (12) leads to

$$\begin{aligned}
&K_1 := \frac{6k_2}{k_1}, \quad K_2 := \frac{3k_3}{k_1}, \quad K_3 := \frac{k_{-1}}{k_1C_0}, \quad K_4 := \frac{k_{-2}}{k_1C_0},\\
&K_5 := \frac{2k_{-3}}{k_1C_0}, \quad K_6 := \frac{k_4}{k_1C_0}, \quad K_7 := \frac{k_{-4}}{k_1C_0}
\end{aligned} \tag{15}$$

the nondimensional formulation of this system

$$\begin{aligned}
\frac{dL}{d\tau} &= K_4C_2 + K_5C_3 - K_1C_1L - K_2C_2L, \\
\frac{dC_1}{d\tau} &= R^2 + K_4C_2 - K_3C_1 - K_1C_1L, \\
\frac{dC_2}{d\tau} &= K_1C_1L + K_5C_3 + K_7C_4 - K_4C_2 - K_6C_2 - K_2C_2L, \\
\frac{dC_3}{d\tau} &= K_2C_2L - K_5C_3, \\
\frac{dC_4}{d\tau} &= K_6C_2 - K_7C_4
\end{aligned} \tag{16}$$

and its corresponding conservation law (13) that will be used to analyse its stability properties

$$R_T = R + 2C_1 + 2C_2 + 2C_3 + 2C_4 \quad \text{with} \quad R_T := \frac{r_T}{C_0}. \tag{17}$$

Stability. Concerning the stability of the system it is important to point out that the positivity issue for the solutions holds true also for the expanded model (16) and can be summarised with the following

Lemma 2.2 (Invariance of the first orthant)**.** *For a non-negative parameter set $K_1, \dots, K_7$ and non-negative initial conditions the solution of the system (16) together with the conservation law (17) remains positive for all times $t \geq 0$.*

Proof. Analogous to the proof of lemma 2.1. □

Computing now the steady states by solving for $\frac{dL}{d\tau} = 0$, $\frac{dC_i}{d\tau} = 0$ $(i = 1, \dots, 4)$ we end up with:

$$C_1 = \frac{R^2}{K_3},\ C_2 = \frac{K_1}{K_3K_4}LR^2,\ C_3 = \frac{K_1K_2}{K_3K_4K_5}L^2R^2,\ C_4 = \frac{K_1K_6}{K_3K_4K_7}LR^2. \tag{18}$$

In order to eliminate the remaining free variables R and L we consider on the one hand the conservation law for the receptors (17) and on the other hand take into account the following conservation law for the ligands that can be derived by adding the first, second, third and fourth equation of (16)

$$0 = \frac{dL}{dt} + \frac{dC_2}{dt} + 2\frac{dC_3}{dt} \implies L_T = L + C_2 + 2C_3 + C_4 \ \text{ with } \ L_T := L(0). \tag{19}$$

Combining then (17) and (19) we arrive at a nonlinear system of equations thus enabling us to identify the steady states of (16). We then investigate their (local) stability by applying linearisation theory and computing the eigenvalues of the corresponding Jacobian

$$\mathrm{J} = \begin{pmatrix} -K_1C_1 - K_2C_2 & -K_1L & K_4 - K_2L & K_5 & 0 \\ -K_1C_1 & -K_1L - K_3 & K_4 & 0 & 0 \\ K_1C_1 - K_2C_2 & K_1L & -K_2L - K_4 & K_5 & K_7 \\ K_2C_2 & 0 & K_2L & -K_5 & 0 \\ 0 & 0 & K_6 & 0 & -K_7 \end{pmatrix}. \tag{20}$$

Contrary to the results in the previous section we cannot fix parameter values for all reaction constants arising in the model, as the values of k_4 and k_{-4} are unknown. Hence we perform a bifurcation analysis by using again the parameter set (10) and varying the value of $K_{D_4} = k_{-4}/k_4$ in order to legitimize the outcome of the numerical simulations in the next section. Figure 6 shows the results of this analysis for fixed values $R_T = 47.5$, $L_T = 1$ and K_{D_4} varying in the range of 10^{-11} to 10^{-1}. Analogously to the previous section, Subfigure (a) shows the the positive part of the (orthogonal projection of the complete steady state vector on the) R component plotted against K_{D_4}, while Subfigure (b) displays the negative part $R < 0$ due to the log-log scaling. Again, the annotations "positive" and "negative" indicate the positivity and negativity of the whole steady state, while the line types dashed and solid denote their stability and instability, respectively.

Concluding from Figure 6 one can see that there exist two stable steady states separated by two unstable steady states. More interestingly, there is only one positive (stable) steady state, hence the expanded model possesses, as well, only one physically relevant equilibrium solution for the considered choice of parameters. Moreover, it can be noted that the steady state of free and unbound receptors R is not affected by the variation of K_{D_4}, as this rate only controls the equilibrium of already bound receptors (and ligands) in the complexes C_2 and C_4, respectively.

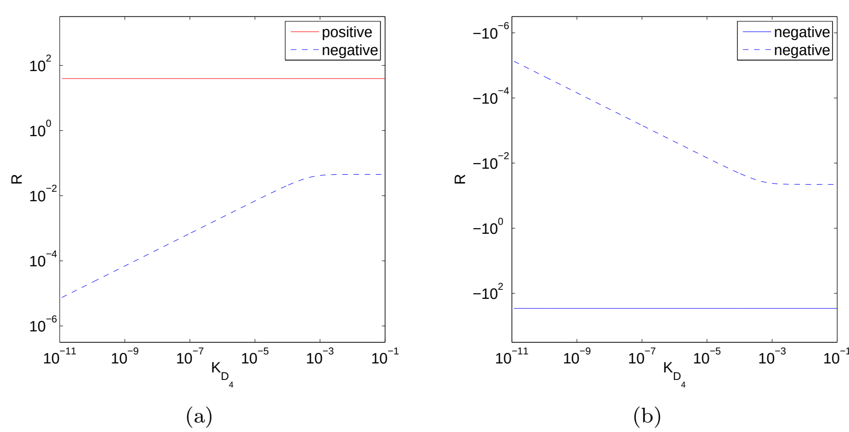

FIGURE 6. Bifurcation diagram for fixed total ligand concentration $L_T = 1$, fixed total receptor concentration $R_T = 47.5$ and varying equilibrium dissociation constant K_{D_4}. Solid and dashed lines indicate the stability and instability of a steady state, while the colours red and blue denote its positivity and negativity, respectively (log-log plot).

3. **Numerical results.**

In this section we present the outcome of the numerical simulations. We begin by explaining how the parameter values for the computations were derived and then demonstrate the impact of their variation on the first and the extended model successively.

Parameter. The parameter values used for the calculations were obtained by evaluating experimental data which are summarized in Table 2 and Table 3. Thereby we considered experimental data of a typical cell death assay consisting of 10 000 cells brought into 200 µL of culture medium. Further we approximated each cell by a sphere with a diameter of 10 µm, estimated the number of receptors per cell with a value of 30 000 and hence arrive at a typical receptor concentration of 9.5×10^{-8} M.

Having now a closer look at the equilibrium dissociation constants $K_{D_i} = k_{-i}/k_i$ accounting for each reaction in the system, observe that we assume a much higher affinity between receptor and ligand than between the receptors themselves, according to data available in the literature [12, 20]. Since for K_{D_4} there do not exist any measured values we vary it over a broad range which should include the real existing value.

Name	Value	Unit	K_D	Unit
k_1	6.0×10^3	$1/\mathrm{M} \cdot \mathrm{min}$	10^{-8},10^{-6},10^{-4}	M
k_{-1}	variable	1/min		
k_2	1.3×10^7	$1/\mathrm{M} \cdot \mathrm{min}$	10^{-10}	M
k_{-2}	1.5×10^{-3}	1/min		
k_3	1.3×10^7	$1/\mathrm{M} \cdot \mathrm{min}$	10^{-10}	M
k_{-3}	1.5×10^{-3}	1/min		
k_4	variable	1/min	10^{-10},10^{-7},10^{-4}	-
k_{-4}	variable	1/min		

TABLE 2. Affinity related parameter set used in the computations (see [12] and [20]).

Name	Lower Value	Upper Value	Unit
l_0	2.0×10^{-14}	2.0×10^{-6}	M
r_T	9.5×10^{-12}	9.5×10^{-6}	M

TABLE 3. Experimental parameter set used in the computations.

First model. The results of the numerical simulations displayed in Figure 7 clarify the impact of the variation of the equilibrium dissociation constant K_{D_1}. From left to right the evolution over the course of time of the concentration of the complexes c_1, c_2 and c_3 with fixed initial data for receptor and ligand concentrations and increasing dissociation constant K_{D_1} is shown in a semilogarithmic plot.

Firstly, note that every component converges as expected to their respective steady state concentration given by the dashed line.

Secondly, the outcomes already indicate that the successful forming of the signalling complex highly depends on the formation of the homodimeric receptor complexes. Particularly, upon observing the order of magnitude of the steady state concentrations for the complexes c_1 and c_2 one can see that in the high affinity case ($K_{D_1} = 10^{-8}$ M) the equilibrium concentrations are more than 10 times higher compared to the ones in the low affinity case ($K_{D_1} = 10^{-4}$ M).

After having looked at some subset of initial receptor and ligand concentrations and the resulting evolution of the cluster concentrations we now want to determine if the behaviour noted so far is preserved by considering a broader range of initial conditions and parameters, as given in Table 3.

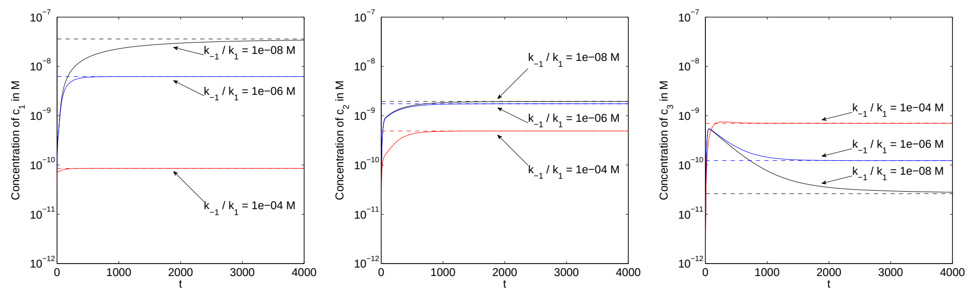

(a) Complex c_1 (b) Complex c_2 (c) Complex c_3

FIGURE 7. Illustration of the cross-linking behaviour for fixed $r_T = 9.5 \times 10^{-8}$ M, fixed $l_0 = 2 \times 10^{-9}$ M and increasing K_{D_1}.

The following Figures 8 to 10 present the results of the calculations carried out using the above mentioned parameter sets. Each of these figures consists of 3 log-log scale plots that differ only in the dissociation constant K_{D_1} used for the calculations (specified in the plots' captions). This implies that each line is always plotted versus the ligand concentration l_0 in the range from 2.0×10^{-14} M to 2.0×10^{-6} M and accounts for only one fixed value r_T of the receptor concentration in the range given by the respective legend. Starting with Figure 8 showing the steady state

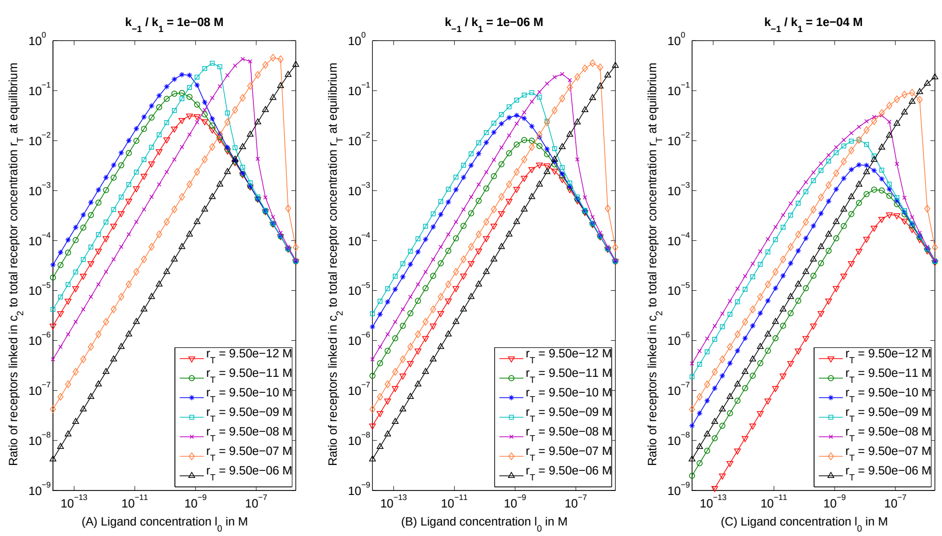

FIGURE 8. Ratio of receptors bound in complex c_2 to total receptor concentration for increasing reaction constant k_{-1} (log-log plot).

ratio of receptors bound in complex c_2 to total receptor concentration r_T versus total ligand concentration l_0, one common observation can be made by examining the results depicted in this figure. It is obvious that the steady state concentration of the complex c_2 increases until the growing ligand concentration l_0 reaches a certain treshold depending on r_T. After that point the concentration of c_2 starts decreasing. This can be explained by the fact that after passing the treshold the concentration of the ligand l_0 reaches a critical value allowing to continue the reaction with c_2 in order to form further complexes of type c_3 and therewith simultaneously to reduce the concentration of c_2.

Figure 9 underlines this assertion by showing a saturation in the ratio of receptors bound in complex c_3 to total receptor concentration r_T. This implies as already mentioned that after the total concentration of the ligand l_0 reaches a critical value almost all remaining complexes of type c_2 turn over into the complex c_3.

Another characteristic common to both reactions is the influence of the increasing equilibrium dissociation constant K_{D_1} in the context of the forming of the homodimeric receptor complex c_1. Clearly, the results of the previous calculations are confirmed, meaning that a low affinity between the receptors results in much lower concentrations of the complexes c_1 and c_2 compared to the high affinity case. In addition, much more ligand is needed to achieve a saturation in signalling complex formation. The results presented in Figure 10 basically sum up all the observations

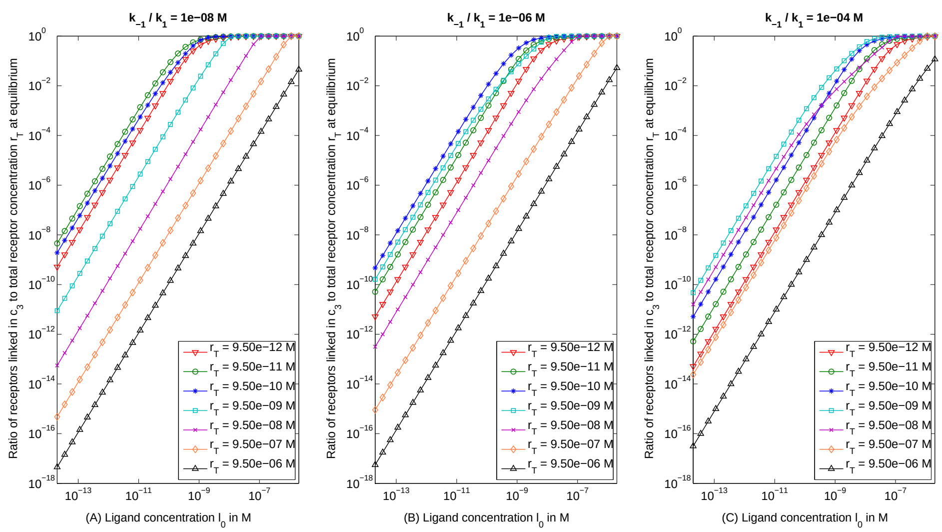

FIGURE 9. Ratio of receptors bound in complex c_3 to total receptor concentration for increasing equilibrium dissociation constant K_{D_1} (log-log plot).

that could be made so far. Thus, the overexpression of ligand does not trigger a substrate inhibition. Contrary, after passing a treshold in the total ligand concentration l_0 a saturation in the formation of the signalling complex occurs. Furthermore, the results suggest that the homodimeric receptor formation plays an important role in the formation of the signalling complex as a variation in the equilibrium dissociation constant resulting in low affinity between the receptors counteracts and therewith delays the formation of signalling complexes.

Extended model. In order to determine the impact of the additional complex c_4 on the system we compute the steady state solutions for the equations (12) with a fixed receptor concentration of 9.5×10^{-8} M, a broad range of ligand concentration and let K_{D_4} vary in the range of 10^{-10} to 10^{-4}. While Figure 11 shows the results

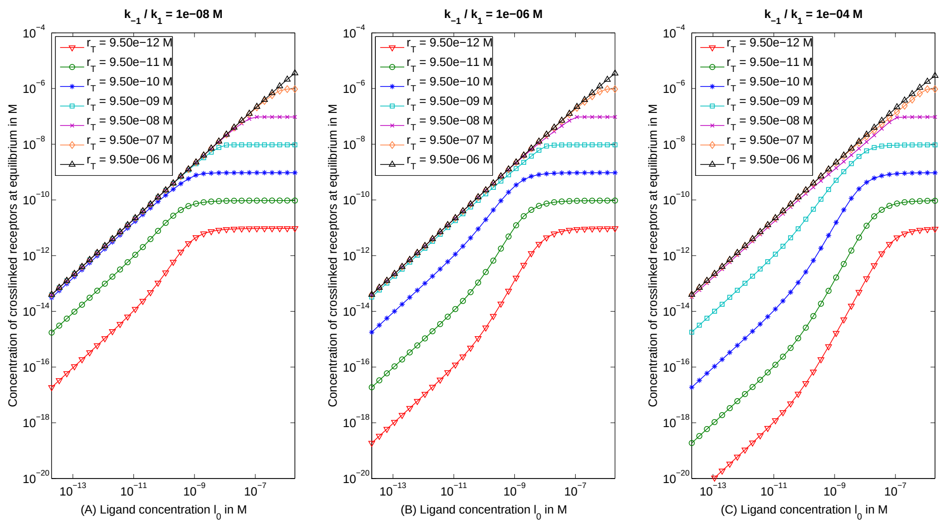

FIGURE 10. Equilibrium cross-linking curve for increasing equilibrium dissociation constant K_{D_1} (log-log plot).

of these computations for the unbound monomeric receptor concentration in comparison to complex c_1, Figure 12 displays the concentrations of the complexes c_1 to c_4 in a log-log scale plot. Clearly, an interesting difference in the behaviour of the system compared to the first model can be noted by the fact that the complex c_3 is no longer the predominant configuration in all cases. Contrary, in the case of high and medium affinity for c_4 (shown in Subfigures (A) and (B)) complex formation is dominated by c_1 for ligand concentrations lower than the receptor concentration (given by the vertical dashed line) and by c_4 after passing that treshold. Only in the case of low affinity (Subfigure (C)) c_3 reaches the highest concentration values. Further we notice from Figure 11 that in all cases there is a strong predominance of the monomeric receptors compared to the dimers in c_1. The biological implications of these observations will be discussed in the next section.

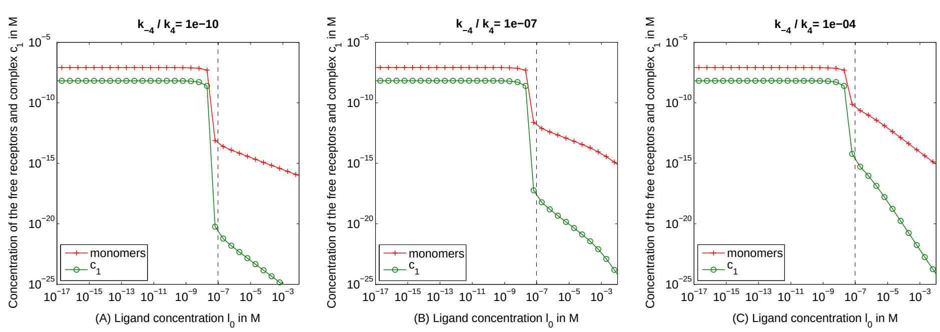

FIGURE 11. Steady state concentrations of unbound receptor monomers and complex c_1 for increasing equilibrium dissociation constant K_{D_4} (log-log plot).

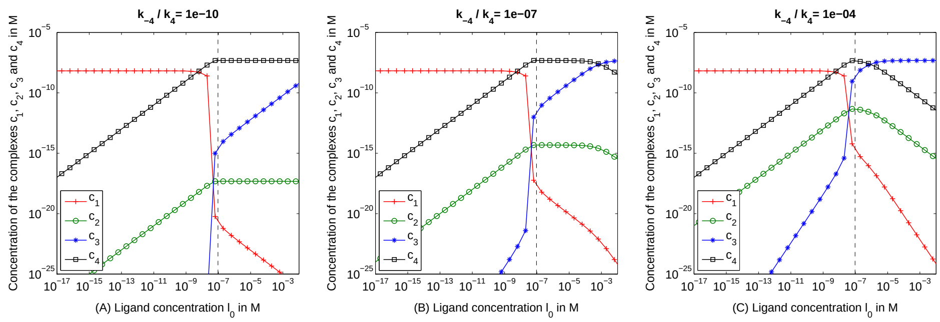

FIGURE 12. Steady state concentrations of complexes c_1 to c_4 for increasing equilibrium dissociation constant K_{D_4} (log-log plot).

4. **Discussion.** In this paper we presented a minimal mathematical model for the initial molecular interactions of death ligands with their cellular membrane receptors. Two distinct molecular interactions are likely to be involved in this process as suggested from literature data. First, regarding ligand/receptor interaction, TNF and several other members of this ligand family have been demonstrated by crystalization studies to form homotrimers, capable to bind three of their respective receptor molecules [3, 15, 25]. In addition, several members of the receptor family, including TNFR1, TNFR2, the four human TRAIL membrane receptors, as well as CD95/Fas, have been shown to form homomultimers in the absence of ligand. Originally formation of homotrimers has been proposed [7], whereas our data strongly suggest preferential homodimer formation in the TNF [6], but also the human TRAIL system (own unpublished data). Furthermore, our own results strongly argue for functional receptor/receptor interactions in the formation of signal competent ligand/receptor clusters [6], as originally proposed by Sprang and coworkers when they observed homodimers upon crystallization of the extracellular domain of TNFR1 [23]. Data available in literature further show that PLAD-mediated homophilic receptor/receptor interactions are of lower affinities as compared to the respective ligand/receptor interactions. Using surface plasmon resonance studies, Lee and coworkers determined association and dissociation rates of homomeric and heteromeric interactions of soluble TRAIL receptors and revealed values for their dissociation constants in the range between one and ten micromolar [20]. Numerous studies exist determining ligand binding affinities of TRAIL to its receptors revealing values for the dissociation constants between 1 nM to 100 nM, as determined by isothermal titration calorimetry [30], isotope-labeled equilibrium binding assays [9] (and own unpublished data) and surface plasmon resonance studies [10, 16]. Similarly, data from equilibrium binding studies [18] as well as association and dissociation studies [12] in the TNF system revealed values for the apparent dissociation constants in the range between 0.1 nM and 10 nM. Accordingly, in our model we chose the reaction rate constants as depicted in Table 2, showing significantly higher affinities for ligand/receptor interaction as compared to the homophilic receptor/receptor interaction.

Additional constraints of our model system are as follows: When the ligand is added, receptors are in an equlilibrium between monomers and dimers which is located far at the side of the monomers, i.e. 86% percent of the receptors exist as monomers and 14% form homodimers. Processes dependent of membrane fluidity are not taken into account, we solely focus on the initial interaction of receptor homodimers with the homotrimeric ligand, resulting in a first step in formation of complex c_2 (Fig. 1). In the next step formation of complex c_3 simply requires binding of one additional ligand, whereas complex c_4 formation is dependent on a major molecular rearrangement in which the PLAD/PLAD interaction of the receptor pair must be opened, but for compensation of this energy demanding step an additional ligand/receptor interaction is formed. Clearly the molecular arrangement of complex c_3 results in a more stable binding of the ligand based on avidity effects. Figure 11 shows the equlibrium between inligated receptor monomers and dimers for three different k_{-4}/k_4 values. It can be seen that with rising ligand concentration depletion of both unligated receptor forms is more efficient in case of a small k_{-4}/k_4 value. Figure 12 depicts the equilibrium concentrations of the complexes c_1 to c_4 as a function of the ligand concentration again calculated for three different k_{-4}/k_4 values. At very low but increasing ligand concentrations in all cases c_2, c_3 and c_4 steadily rise at the expense of the unligated receptors (Fig. 11). The dotted vertical line indicates where the ligand trimer concentration equals that of the total receptor concentration. Clearly, this is the ligand concentration range where major changes in the concentrations of complexes can be observed. At this point the system is dominated by complex c_4 but a further increase in the ligand concentration leads to a rising in the complex c_3. Dependent on the chosen values for k_{-4}/k_4 finally the complex c_3 becomes the predominant form with steadily decreasing concentrations of complexes c_1, c_2 and c_4, as well as the unligated receptors.

Interesting biological questions rise from our model, predicting that the system is dominated by complex c_3 at very high ligand concentrations. Importantly, if all receptors are trapped in complex c_3, formation of ligand/receptor clusters must be blocked due to the lack of interaction partners for the receptor bound ligands. Further, crystallisation studies from the unligated extracellular domain of TNFR1 and its complex with the TNF homologue lymphotoxin alpha revealed no major conformational differences between these receptor chains. This strongly suggests that complex c_3 as such is not signalling competent as is the unligated receptor dimer, which is in accordance with the mentioned hypothesis of signalling clusters. Accordingly, complex c_3 most likely represents a signalling incompetent end point of the receptors at extremely high ligand concentrations, meaning that death ligands principally show the phenomenon of excess substrate inhibition. However, we are not aware of any description of substrate (ligand) inhibition of any TNF family member and also in our own experiments we were unable to detect it. No excess ligand inhibition could be observed when we applied TNF concentrations up to 80 nM in an established system [17] of TNF-driven apoptosis (data not shown). Physiological serum TNF concentrations in healthy individuums are well beyond 20 pM and remain in the lower nM range even in the case of a life threatening septic shock [31]. So one can generally assume that (patho)physiological cellular responses are initiated already by TNF concentrations in the higher pM range. At these concentrations, however, our model clearly predicts that the system is dominanted by the complexes c_2 and c_4 over a broad range of k_{-4}/k_4 (Fig. 5 and Fig. 12). A significant appearance of c_3 (in the order of 10 percent of total receptors) would occur at a ligand concentration above 10^{-7} M even under advantageous conditions with a k_{-4}/k_4 value of 10^{-4}. Together, we conclude that the formation of complex c_3, which should cause the phenomenon of substrate inhibition, is not of importance under physiological conditions.

In a recent publication Lai and Jackson have also constructed and analysed a mathematical model for signalling of the death receptor Fas. In contrast to our approach these authors assumed that the ligand homotrimer bound to three receptor chains represents the actual signalling complex. Interestingly, from their model it was concluded that a strong substrate inhibition would occur at ligand concentrations above that of the dissociation constant value [19]. As excess ligand inhibition does not appear to play a major role in death receptor signalling, we take the results obtained by Lai and Jackson as a further indication that complexes comprising one ligand trimer and three receptor chains are not capable to signal.

REFERENCES

[1] B. B. Aggarwal, *Signalling pathways of the TNF superfamily: A double-edged sword*, Nature Reviews Immunology, **3** (2003), 745–756.

[2] Hyun-Jung An, Young Jin Kim, Dong Hyun Song, Beom Suk Park, Ho Min Kim, Ju Dong Lee, Sang-Gi Paik, Jie-Oh Lee and Hayyoung Lee, *Crystallographic and mutational analysis of the CD40-CD154 complex and its implications for receptor activation*, Journal of Biological Chemistry, **286** (2011), 11226–11235.

[3] David W. Banner, Allan D'Arcy, Wolfgang Janes, Reiner Gentz, Hans-Joachim Schoenfeld, Clemens Broger, Hansruedi Loetscher and Werner Lesslauer, *Crystal structure of the soluble human 55 kd TNF receptor-human TNF[beta] complex: Implications for TNF receptor activation*, Cell, **73** (1993), 431–445.

[4] D. Berg, M. Lehne, N. Müller, D. Siegmund, S. Münkel, W. Sebald, K. Pfizenmaier and H. Wajant, *Enforced covalent trimerization increases the activity of the TNF ligand family members TRAIL and CD95L*, Cell Death and Differentiation, **14** (2007), 2021–2034.

[5] Verena Boschert, Anja Krippner-Heidenreich, Marcus Branschädel, Jessica Tepperink, Andrew Aird and Peter Scheurich, *Single chain TNF derivatives with individually mutated receptor binding sites reveal differential stoichiometry of ligand receptor complex formation for TNFR1 and TNFR2*, Cellular Signalling, **22** (2010), 1088–1096.

[6] Marcus Branschädel, Andrew Aird, Andrea Zappe, Carsten Tietz, Anja Krippner-Heidenreich and Peter Scheurich, *Dual function of cysteine rich domain (CRD) 1 of TNF receptor type 1: Conformational stabilization of CRD2 and control of receptor responsiveness*, Cellular Signalling, **22** (2010), 404–414.

[7] Francis Ka-Ming Chan, Hyung J. Chun, Lixin Zheng, Richard M. Siegel, Kimmie L. Bui and Michael J. Lenardo, *A domain in TNF receptors that mediates ligand-independent receptor assembly and signaling*, Science, **288** (2000), 2351–2354.

[8] Lauren Clancy, Karen Mruk, Kristina Archer, Melissa Woelfel, Juthathip Mongkolsapaya, Gavin Screaton, Michael J. Lenardo and Francis Ka-Ming Chan, *Preligand assembly domain-mediated ligand-independent association between TRAIL receptor 4 (TR4) and TR2 regulates TRAIL-induced apoptosis*, Proceedings of the National Academy of Sciences of the USA, **102** (2005), 18099–18104.

[9] M. A. Degli-Esposti, M. C. Dougall, P. J. Smolak, J. Y. Waugh, C. A. Smith and R. G. Goodwin, *The novel receptor TRAIL-R4 induces NF-kappaB and protects against TRAIL-mediated apoptosis, yet retains an incomplete death domain*, Immunity, **7** (1997), 813–820.

[10] John G. Emery, Peter McDonnell, Michael Brigham Burke, Keith C. Deen, Sally Lyn, Carol Silverman, Edward Dul, Edward R. Appelbaum, Chris Eichman, Rocco DiPrinzio, Robert A. Dodds, Ian E. James, Martin Rosenberg, John C. Lee and Peter R. Young, *Osteoprotegerin is a receptor for the cytotoxic ligand TRAIL*, Journal of Biological Chemistry, **273** (1998), 14363–14367.

[11] Matthias Grell, Eleni Douni, Harald Wajant, Matthias Löhden, Matthias Clauss, Beate Maxeiner, Spiros Georgopoulos, Werner Lesslauer, George Kollias, Klaus Pfizenmaier and Peter Scheurich, *The transmembrane form of tumor necrosis factor is the prime activating ligand of the 80 kDa tumor necrosis factor receptor*, Cell, **83** (1995), 793–802.

[12] Matthias Grell, Harald Wajant, Gudrun Zimmermann and Peter Scheurich, *The type 1 receptor (CD120a) is the high-affinity receptor for soluble tumor necrosis factor*, Proceedings of the National Academy of Sciences of the United States of America, **95** (1998), 570–575.

[13] F. Henkler, E. Behrle, K. M. Dennehy, A. Wicovsky, N. Peters, C. Warnke, K. Pfizenmaier and H. Wajant, *The extracellular domains of Fasl and Fas are sufficient for the formation*

of supramolecular FasL-Fas clusters of high stability, Journal of Cell Biology, **168** (2005), 1087–1098.

[14] N. Holler, A. Tardivel, M. Kovacsovics-Bankowski, S. Hertig, O. Gaide, F. Martinon, A. Tinel, D. Deperthes, S. Calderara, T. Schulthess, J. Engel, P. Schneider and E. Tschopp, *Two adjacent trimeric Fas ligands are required for Fas signaling and formation of a death-inducing signaling complex*, Molecular And Cellular Biology, **23** (2003), 1428–1440.

[15] Sarah G. Hymowitz, Hans W. Christinger, Germaine Fuh, Mark Ultsch, Mark O'Connell, Robert F. Kelley, Avi Ashkenazi and Abraham M. de Vos, *Triggering cell death: The crystal structure of apo2l/TRAIL in a complex with death receptor 5*, Molecular Cell, **4** (1999), 563–571.

[16] Sarah G. Hymowitz, Mark P. O'Connell, Mark H. Ultsch, Amy Hurst, Klara Totpal, Avi Ashkenazi, Abraham M. de Vos and Robert F. Kelley, *A unique zinc-binding site revealed by a high-resolution x-ray structure of homotrimeric Apo2L/TRAIL*, Biochemistry, **39** (2000), 633–640.

[17] A. Krippner-Heidenreich, F. Tübing, S. Bryde, S. Willi, G. Zimmermann and P. Scheurich, *Control of receptor-induced signaling complex formation by the kinetics of ligand/receptor interaction*, Journal of Biological Chemistry, **277** (2002), 44155–44163.

[18] F. C. Kull, S. Jacobs and P. Cuatrecasas, *Cellular receptor for 125I-labeled tumor necrosis factor: Specific binding, affinity labeling, and relationship to sensitivity*, Proceedings of the National Academy of Sciences of the United States of America, **82** (1985), 5756–5760.

[19] R. Lai and T. L. Jackson, *A mathematical model of receptor-mediated apoptosis: Dying to know why FasL is a trimer*, Mathematical Biosciences and Engineering, **1** (2004), 325–338.

[20] H. W. Lee, S. H. Lee, Y. W. Ryu, M. H. Kwon and Y. S. Kim, *Homomeric and heteromeric interactions of the extracellular domains of death receptors and death decoy receptors*, Biochemical and Biophysical Research Communications, **330** (2005), 1205–1212.

[21] Frank Mühlenbeck, Pascal Schneider, Jean-Luc Bodmer, Ralph Schwenzer, Angelika Hauser, Gisela Schubert, Peter Scheurich, Dieter Moosmayer, Jürg Tschopp and Harald Wajant, *The tumor necrosis factor-related apoptosis-inducing ligand receptors TRAIL-R1 and TRAIL-R2 have distinct cross-linking requirements for Initiation of apoptosis and are non-redundant in JNK activation*, Journal of Biological Chemistry, **275** (2000), 32208–32213.

[22] Y. Mukai, T. Nakamura, M. Yoshikawa, Y. Yoshioka, S. Tsunoda, S. Nakagawa, Y. Yamagata and Y. Tsutsumi, *Solution of the structure of the TNF-TNFR2 complex*, Science Signaling, **3** (2010), ra83.

[23] James H. Naismith, Tracey Q. Devine, Barbara J. Brandhuber and Stephen R. Sprang, *Crystallographic evidence for dimerization of unliganded tumor necrosis factor receptor*, Journal of Biological Chemistry, **270** (1995), 13303–13307.

[24] James H. Naismith, Tracey Q. Devine, Tadahiko Kohno and Stephen R. Sprang, *Structures of the extracellular domain of the type I tumor necrosis factor receptor*, Structure, **4** (1996), 1251–1262.

[25] P. Schneider, J. L. Bodmer, N. Holler, C. Mattmann, P. Scuderi, A. Terskikh, M. C. Peitsch and J. Tschopp, *Characterization of Fas (Apo-1, CD95)-Fas ligand interaction*, Journal of Biological Chemistry, **272** (1997), 18827–18833.

[26] P. Schneider, N. Holler, J. L. Bodmer, M. Hahne, K. Frei, A. Fontana and J. Tschopp, *Conversion of membrane-bound Fas ligand to its soluble form is associated with down regulation of its proapoptotic activity and loss of liver toxicity*, Journal of Experimental Medicine, **187** (1998), 1205–1213.

[27] Richard M. Siegel, John K. Frederiksen, David A. Zacharias, Francis Ka-Ming Chan, Michele Johnson, David Lynch, Roger Y. Tsien and Michael J. Lenardo, *Fas preassociation required for apoptosis signaling and dominant inhibition by pathogenic mutations*, Science, **288** (2000), 2354–2357.

[28] Richard M. Siegel, Jagan R. Muppidi, Malabika Sarker, Adrian Lobito, Melinda Jen, David Martin, Stephen E. Straus and Michael J. Lenardo, *SPOTS: Signaling protein oligomeric transduction structures are early mediators of death receptor-induced apoptosis at the plasma membrane*, The Journal of Cell Biology, **167** (2004), 735–744.

[29] Steven H. Strogatz, "Nonlinear Dynamics and Chaos: With Applications to Physics, Biology, Chemistry and Engineering," 1^{st} edition, Perseus Books, Cambridge, Massachusetts, 1994.

[30] Alemseged Truneh, Sunita Sharma, Carol Silverman, Sanjay Khandekar, Manjula P. Reddy, Keith C. Deen, Megan M. McLaughlin, Srinivasa M. Srinivasula, George P. Livi, Lisa A. Marshall, Emad S. Alnemri, William V. Williams and Michael L. Doyle, *Temperature-sensitive*

differential affinity of TRAIL for its receptors. DR5 is the highest affinity receptor, Journal of Biological Chemistry, **275** (2000), 23319–23325.

[31] A. Waage, P. Brandtzaeg, A. Halstensen, P. Kierulf and T. Espevik, *The complex pattern of cytokines in serum from patients with meningococcal septic shock. association between interleukin 6, interleukin 1, and fatal outcome*, Journal of Experimental Medicine, **169** (1989), 333–338.

[32] Harald Wajant, Dieter Moosmayer, Thomas Wüest, Till Bartke, Elke Gerlach, Ulrike Schönherr, Nathalie Peters, Peter Scheurich and Klaus Pfizenmaier, *Differential activation of TRAIL-R1 and -2 by soluble and membrane TRAIL allows selective surface antigen-directed activation of TRAIL-R2 by a soluble TRAIL derivative*, Oncogene, **20** (2001), 4101–4106.

[33] Wolfgang Walter, "Gewöhnliche Differentialgleichungen. Eine Einführung," 6^{th} edition, Springer-Verlag, Berlin, 1996.

[34] Liwei Wang, Jin Kuk Yang, Venkataraman Kabaleeswaran, Amanda J. Rice, Anthony C. Cruz, Ah Young Park, Qian Yin, Ermelinda Damko, Se Bok Jang, Stefan Raunser, Carol V. Robinson, Richard M. Siegel, Thomas Walz and Hao Wu, *The Fas-FADD death domain complex structure reveals the basis of DISC assembly and disease mutations*, Nature Structural & Molecular Biology, **17** (2010), 1324–1329.

Received August 8, 2011; Accepted May 14, 2012.

E-mail address: christian.winkel@mathematik.uni-stuttgart.de
E-mail address: simon.neumann@izi.uni-stuttgart.de
E-mail address: christina.surulescu@uni-muenster.de
E-mail address: peter.scheurich@izi.uni-stuttgart.de